SAND2016-11534C

Design and Implementation of a Wide-Area Damping Controller Using High Voltage DC Modulation and Synchrophasor Feedback*

David A. Schoenwald Brian J. Pierre** Felipe Wilches-Bernal** Daniel J. Trudnowski*****

***Sandia National Laboratories, Albuquerque, NM 87185 USA*
(e-mails: {daschoe,bjpierr,fwilche}@sandia.gov)
****Montana Tech, Butte, MT 59701 USA (e-mail: dtrudnowski@mtech.edu)*

Abstract: This paper describes the design strategy and testing results of a control system to improve damping of inter-area oscillations in the western North American Power System (wNAPS) in order to maintain dynamic stability of the grid. Extensive simulation studies and actual test results on the wNAPS demonstrate significant improvements in damping of inter-area oscillations of most concern without reducing damping of peripheral oscillations. The design strategy of the control system features three novel attributes: (1) The feedback law for the control system is constructed using real-time measurements acquired from Phasor Measurement Units (PMUs) located throughout the power grid. (2) Control actuation is delivered by the modulation of real power flow through a High Voltage Direct Current (HVDC) transmission line. (3) A supervisory system, integrated into the control system is in charge of determining damping effectiveness, maintaining failsafe operation, and ensuring that no harm is done to the grid.

Keywords: Power systems stability; Smart grids; Monitoring and control of spatially distributed systems; Dynamic interaction of power plants; Control under communication constraints; Integrated monitoring, security and control of critical infrastructure systems.

1. INTRODUCTION

A collaboration of technical staff from Sandia National Laboratories (SNL), Montana Tech University (MTU), and the Bonneville Power Administration (BPA) has developed a control system for active damping of north-south oscillations in the western North American Power System (wNAPS). The control system acquires voltage measurements from Phasor Measurement Units (PMUs) located throughout the BPA region. These measurements provide feedback information necessary for the control system to construct a commanded power signal. This power command is then used to modulate the Pacific DC Intertie (PDCI) by as much as ±125 MW of its 3220 MW rated capacity.

A major milestone was achieved on 29 Sept. 2016 when the control system was tested in closed-loop operation on the PDCI for the first time. These tests were conducted in coordination with BPA, the Los Angeles Department of Water and Power (LADWP), and the Western Electricity Coordinating Council (WECC). Test results showed significant improvement in damping of the primary north-south oscillation mode when the control system was active in comparison to when it was inactive. These results were achieved without reducing the damping of other oscillation modes or otherwise causing any deleterious effects in the wNAPS. This is the first instance in which PMU measurements have been deployed for real-time feedback control on a wide-area power grid in North America.

The concept of modulating a major HVDC transmission line to damp inter-area oscillations is not new. Modulation of the PDCI for damping control was first prototyped in the 1970s as described in Cresap et al. (1978). Review of this work via reports and oral interviews with engineers in charge of the project revealed two primary conclusions. First, the HVDC modulation improved inter-area mode damping considerably. Second, the feedback signal, which was derived from a localized AC power flow, resulted in a right half plane zero in the system transfer function. The second issue resulted in the controller worsening higher frequency inter-area oscillations in the wNAPS. Despite the improvement in damping to the north-south modes, the destabilizing effect on other modes was an unacceptable trade-off. This issue was the primary reason that the control strategy did not become operational. For additional details, see Kosterev et al. (1999).

One of the most important design features incorporated in the damping controller described in this paper is the use of real-time data from Phasor Measurement Units (PMUs) for feedback control, detailed in Pierre et al. (2016) and Trudnowski et al. (2013). This feedback information is used to estimate a relative frequency signal that forms the basis for the modulation power command.

PMUs transmit satellite-synchronized time and location stamped measurements over communication networks at high data rates (typically 60 Hz). With the acquisition and processing of PMU data over a power grid, one can now get a much more accurate and up to date picture of oscillatory dy-

*The authors gratefully acknowledge financial support for this project from the Bonneville Power Administration (BPA) Office of Technology Innovation and the U.S. Department of Energy Office of Electricity (DOE/OE) Transmission Reliability and Energy Storage programs.
**Sandia National Laboratories is a multi-mission laboratory managed and operated by Sandia Corporation, a wholly owned subsidiary of Lockheed Martin Corporation, for the US Department of Energy's National Nuclear Security Administration, under contract DE-AC04-94AL85000.

namics in the power grid. With the real-time use of this information, the threat of unintended destabilization of any oscillatory modes in the grid can be greatly reduced. For additional details, see Trudnowski et al. (2013).

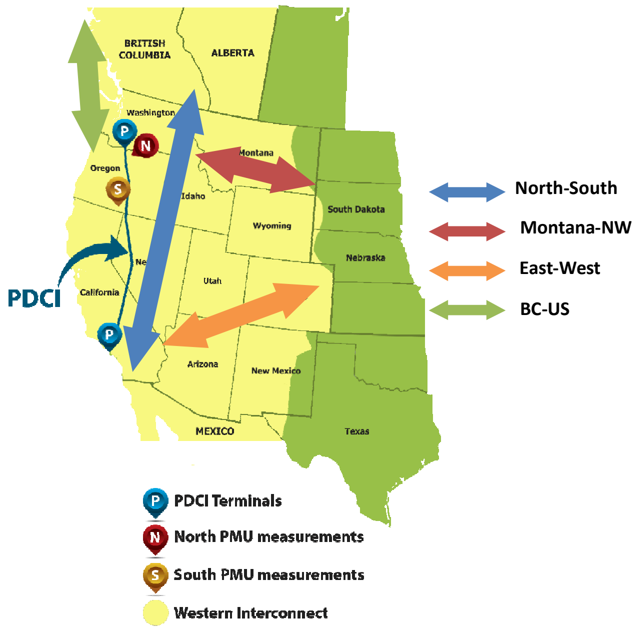

Fig. 1. Map of the western North American Power System (wNAPS) showing location of Pacific DC Intertie (PDCI), PMU locations, and inter-area modes of oscillation.

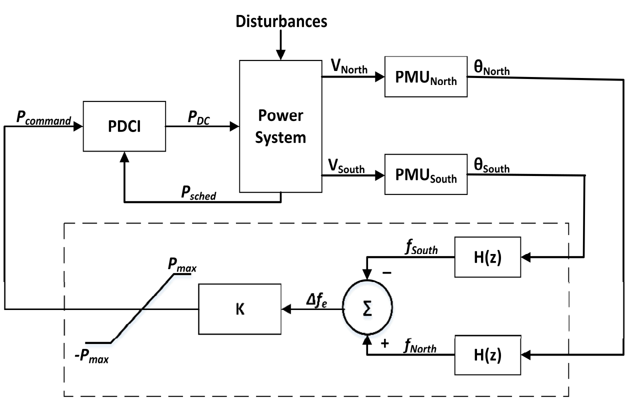

Fig. 2. Block diagram of damping controller.

Substantial effort has been invested by the project team to ensure that the control system causes no harm to the grid under all possible operating conditions. Further, the controller must successfully operate despite variabilities and uncertainties in PMU network latencies. To ensure these key objectives are satisfied, the project team developed a supervisory system that continuously monitors grid conditions, PMU data characteristics, the PDCI status, and controller hardware status. The monitoring informs a set of flags, which can alarm if any threshold boundaries are exceeded. If any of the flags reaches an alarm state then the controller ceases active operation in a bumpless fashion. For additional details on the supervisory system, see Pierre et al. (2016).

2. CONTROL STRATEGY

The damping control strategy is a proportional action on the frequency difference of two separate areas of the wNAPS. One of the frequency measurements is acquired from the northern part of the wNAPS and the other is acquired from the southern part of the wNAPS.

This control strategy is modeled by

$$P_{command} = K\big(f_{North}(t-\tau_{d1}) - f_{South}(t-\tau_{d2})\big). \quad (1)$$

In (1), K is typically in units of MW/mHz, f_{North} and f_{South} are computed using appropriately selected PMUs in the north and south respectively, and τ_{d1}, τ_{d2} are the time delays associated with the PMU data network. The resulting power command signal is then dispatched to the PDCI controls located at the northern terminal of the PDCI. This control strategy adds damping to the primary north-south oscillatory modes in the wNAPS without reducing the damping of other modes of oscillation in the wNAPS. Fig. 1 illustrates the primary inter-area modes of oscillation in the wNAPS.

In practice, the controller samples the electrical bus angles $\theta_{North}(t)$ and $\theta_{South}(t)$ from appropriately selected PMU locations and applies a derivative filter, $H(z)$, to each angle measurement to attain a frequency difference between the north and south measurements $\Delta f_e(t)$. Further, the time delays, $\tau_{d1} = \tau_{d2}$, because the controller time aligns the North and South bus angles such that measurements taken at the same time instant are used in the control law. A proportional gain K and saturation limits (normally +/-125 MW) are applied to this signal yielding the commanded power modulation in MW. The overall control strategy is depicted in Fig. 2.

The derivative filter was designed such that the controller could effectively damp inter-area oscillations between 0.2 and 1.0 Hz. Oscillations outside this frequency range are significantly attenuated. The derivative filter is modeled by the transfer function,

$$H(z) = \frac{0.292 - 0.292z^{-2}}{1 - 1.557z^{-1} + 0.618z^{-2}}. \quad (2)$$

This transfer function represents a 2nd-order Bessel filter cascaded with a derivative operation based on Tustin's approximation. This control design minimizes filter delay while still adding significant damping to the primary north-south oscillatory mode in the wNAPS without exciting or otherwise interfering with higher frequency bands. Minimizing the impact of time delays on control performance has been a high priority throughout the control design process. In particular, time delays associated with network latencies in acquiring PMU data can be stochastic in nature and if excessive, can lead to unstable control, as in Stahlhut et al. (2008).

3. MODELING AND SIMULATION RESULTS

Multiple levels of fidelity in modelling the wNAPS are incorporated in the simulation of the control system. To demonstrate proof-of-concept, the initial control design was simulated on the two-area model from Kundur (1994) as shown in Fig. 3. Next, a higher order model of the wNAPS, based in MATLAB and originally developed and validated in

Trudnowski and Undrill (2009), was used to simulate the control design. The one-line diagram for this model is illustrated in Fig. 4. Finally, a high fidelity model of the wNAPS, adapted from a model specifically developed and validated by WECC, was used to simulate the control design.

The high fidelity model uses the GE Positive Sequence Load Flow (PSLF) software as its simulation platform. The specific WECC-developed model adapted for the simulation studies was the heavy summer 2016 base case. This base case models 31,419 buses, 4063 generators, 22,813 branches, and 10,748 loads. To adapt this model for simulation of the damping controller, a custom transient stability model was developed in PSLF to incorporate the PDCI-based damping controller illustrated in Fig. 2 along with the dynamics of the PDCI itself. Validation of the PDCI dynamics, determined by analysis of probing tests, is described in Trudnowski et al. (2014).

Hundreds of simulations were conducted to evaluate grid performance both with and without the damping controller, consistently showing improved performance for the latter case. Figs. 5-7 depict the simulation of a Chief Joseph Brake (CJB) insertion for 1 sec duration. The CJB is a dynamic braking resistor capable of producing an additional load on the grid of 1.4 GW for time durations between 0.5 to 4 secs. The CJB, located at the Chief Joseph substation in Washington State, USA, is detailed in Shelton et al. (1975).

Two simulations are compared here, no control vs. control with a gain, K = 12 MW/mHz. The frequency difference between the north PMU and the south PMU is significantly damped with control vs. no control, as shown in Fig. 5. Fig. 6 shows the frequency response to the CJB event at specific buses in the wNAPS. The system recovers to the pre-disturbance steady-state frequency as expected. During the event, the controller modulates PDCI power, shown in Fig. 7.

Using Prony analysis, as described in Trudnowski and Pierre (2009), damping of the primary north-south mode can be computed. There is a 51% improvement in damping with control using K = 12 MW/mHz vs. no control (12.4% damping vs. 8.2% damping), shown in Table 1. The amount of damping improvement demonstrated by these simulations is significant. Analysis of actual test results conducted on the PDCI (see Section 5) demonstrate a very similar amount of damping improvement for operating conditions that closely approximate those modeled by the simulations.

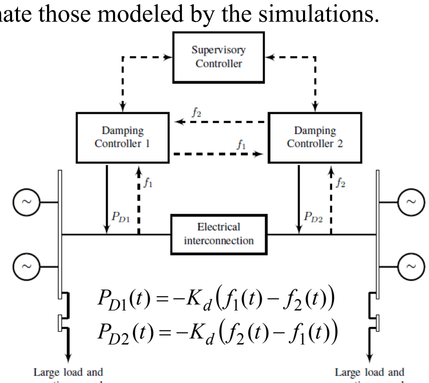

Fig. 3. Adaptation of two-area model in Kundur (1994) for use in simulation analysis of damping controller.

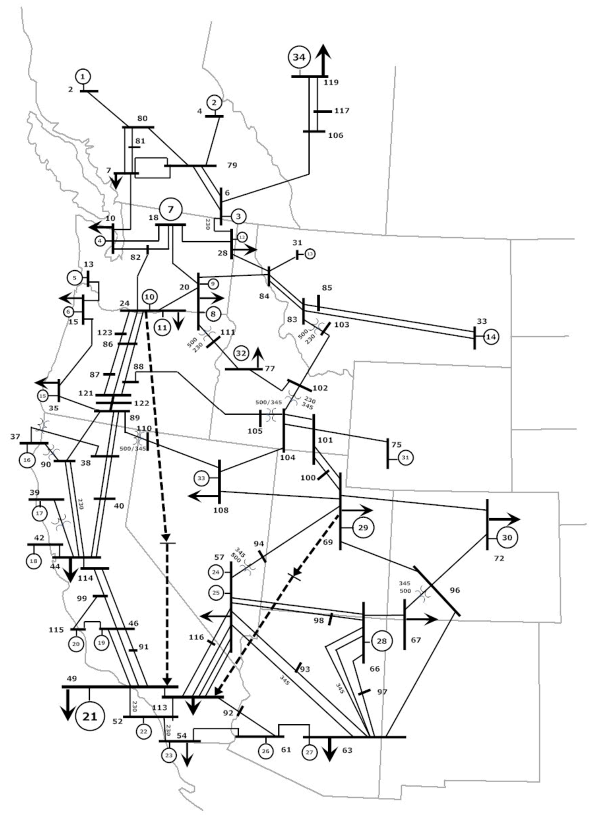

Fig. 4. Simplified one-line of the wNAPS from Trudnowski and Undrill (2009).

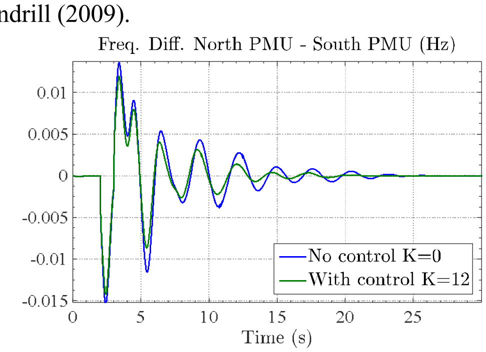

Fig 5. Frequency difference between north PMU location and south PMU location during a CJB insertion.

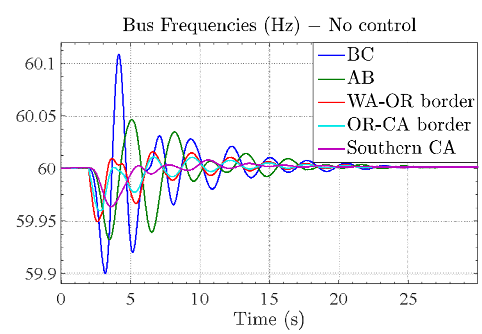

Fig. 6. Bus frequencies during a CJB insertion for one second in British Columbia (BC), Alberta (AB), the Washington-Oregon (WA-OR) border, the Oregon-California (OR-CA) border, and in southern California (CA).

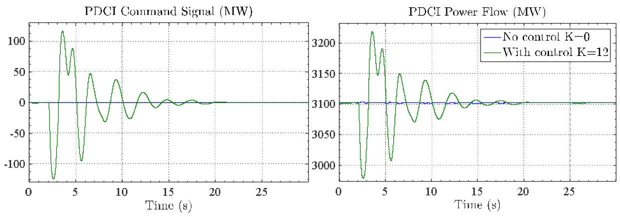

Fig 7. The controller commanded power (P_{command}) and the power flow on the PDCI (P_{DC}) during a CJB insertion.

Table 1. NSB mode damping results from simulation of a Chief Joseph Brake insertion for one second

	NSB mode	
	Mode frequency	% Damping
No control	0.363 Hz	8.2%
Control with gain 12 MW/mHz	0.366 Hz	12.4%

4. HARDWARE AND SUPERVISORY SYSTEM

A hardware prototype was constructed to implement the control scheme as seen in Fig. 8. Therein, three key subsystems are shown, including the Watchdog module, Real-time controller, and the Asynchronous server. The KVM switch and monitor are for the user interface.

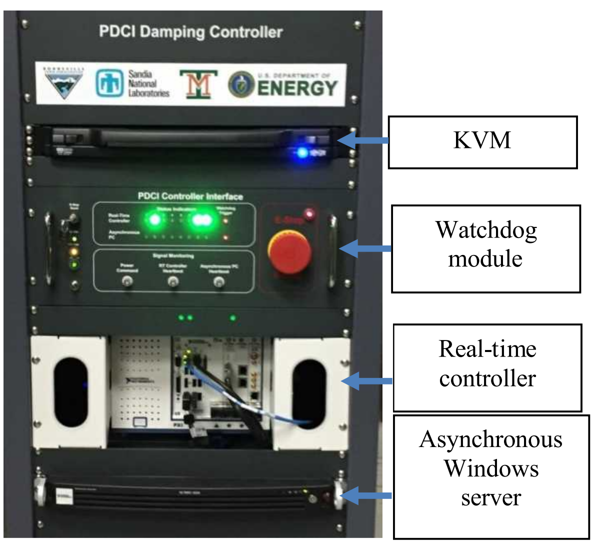

Fig. 8. Photograph of damping controller hardware.

The real-time damping controller and asynchronous monitor are implemented on National Instruments (NI) computer platforms. The damping controller software is run within a real-time operating system on the NI PXI-8135, which is housed in an NI PXI chassis with an NI PXIe-5341 multi-function I/O module. A +/-10V analogue command signal is generated by this module to represent the commanded power order, which is converted into MWs. The asynchronous monitor is implemented on-board an NI RMC-8354 server. Both platforms generate a heartbeat signal that is monitored by the hardware interface. The hardware interface includes watchdog circuits, an E-stop circuit, and mechanical relays that connect the analogue signal to the PDCI controller input.

To ensure safe and reliable performance, the project integrates a supervisory system to ensure the controller is operating as expected at all times. A suite of supervisory functions is implemented across the three hardware platforms. The real-time controller includes several checks on the PMU data and performance, communications delays, network-operating conditions, and the wNAPS conditions. The asynchronous server includes automated probing, transfer function estimation, gain and phase margin monitoring, and PDCI monitoring (this is still under development). Lastly, the Watchdog module is used to check the control interface itself. If either platform stops running (heartbeat stops), or if a malfunction or noncompliant behaviour is detected by the watchdog circuit, or if the E-stop button is pressed by an operator, the analogue signal from the damping controller is interrupted by opening a relay. Then, the voltage signal provided to the PDCI control is ramped to zero via bumpless transfer.

When a change in system state is necessary, the damping controller utilizes a bumpless transfer to eliminate step functions in the control signal. For example, when the controller is disabled the command signal does not immediately go to zero, rather it ramps down to zero at a specified rate as in Fig. 9. In addition, the controller looks for a zero crossing when connecting the command signal to the PDCI as in Fig. 10.

The controller also utilizes PMU redundancy to improve system reliability. The controller uses four PMU measurements from the north and four from the south. These eight PMU measurements allow the controller to run 16 parallel control instances that are prioritized by the best possible PMU pair. Each controller instance takes data from a single north PMU and a single south PMU and outputs a real power modulation signal, P_{command}. To enable seamless switching between PMU pairs, the controller again utilizes bumpless transfer.

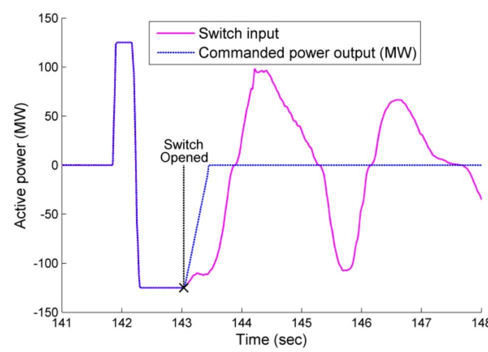

Fig. 9. Controller ramps command to zero to disable control.

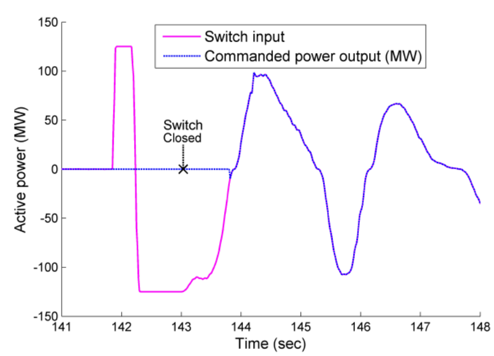

Fig. 10. Controller identifies zero crossing to enable control.

5. RESULTS FROM TESTING ON THE PDCI

Testing of the damping controller in closed-loop operation was conducted on 29 Sept. 2016. In order to adequately test the performance of the damping controller, tests were conducted in both open loop and closed loop operation in which exogenous inputs were injected to the grid. Comparison of open and closed loop tests with Chief Joseph Brake Pulses is one of the most effective means to determine the impact of the damping controller on inter-area oscillations. These brake pulses are essentially impulse inputs to the grid, resulting in a strong response from inter-area modes of oscillation.

The closed-loop test inserts a Chief Joseph Brake Pulse at time = 1 sec. The damping controller modulates the PDCI with a medium gain. The primary north-south mode damping is 15.7% (calculated using Prony's method). The open-loop test inserts a Chief Joseph Brake Pulse also at time = 1 sec. The damping controller is inactive during this test. The primary north-south mode damping is 11.2% (calculated using Prony's method). Thus, the damping values for the primary north-south mode show a 4.5 percentage point improvement, which is significant. The remaining oscillatory modes in the wNAPS also showed small improvements in damping.

Figs. 11-13 illustrate the response to Chief Joseph Brake Pulses of inter-area oscillations, north and south grid frequencies, and PDCI power output, respectively, in both open and closed loop damping control operation. For the power flow on the PDCI depicted in Fig. 13, the closed-loop plot shows the addition of the PDCI power flow and the commanded power modulation dispatched to the PDCI. The open-loop plot shows only the PDCI power flow since the commanded modulated power is zero in open-loop operation.

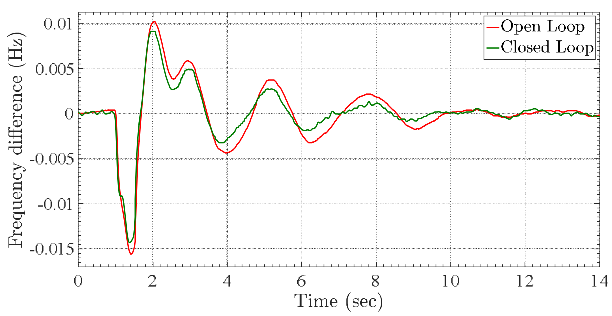

Fig. 11. Difference in north and south PMU frequencies in open & closed loop during a CJB insertion on 29 Sept. 2016.

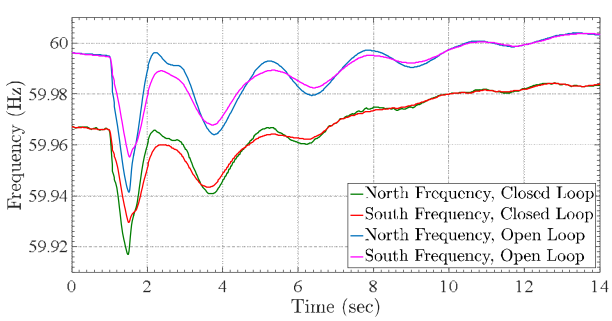

Fig. 12. PMU frequencies from north and south locations in open & closed loop during a CJB insertion on 29 Sept. 2016.

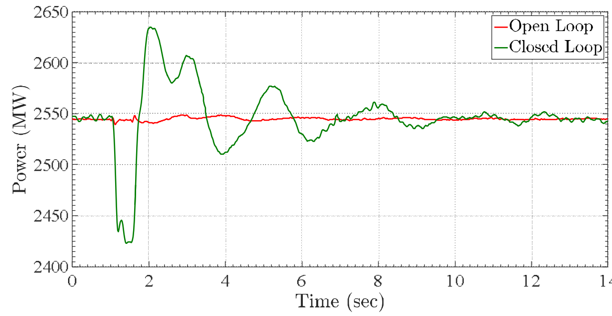

Fig. 13. The power flow on the PDCI during a CJB insertion on 29 Sept. 2016.

The closed loop test inserts 3 periods of a square wave (7.5 sec at 2.5 sec/pulse – 0.4 Hz, amplitude = +/- 125 MW) onto the PDCI via the Probing Signal Generator (PSG), independent of the damping controller at time = 1 sec. The damping controller modulates the PDCI with a high gain.

The open loop test inserts 3 periods of a 0.4 Hz square wave with amplitude = ±125 MW onto the PDCI via the PSG, which is again independent of the damping controller, at time = 1 sec. The damping controller is inactive during this test.

Comparing the open and closed loop results, the damping controller significantly reduces the north-south inter-area oscillation in about 15 seconds. For the open loop case, it takes an additional 8 seconds to achieve approximately the same reduction in oscillation amplitude. Note that the square wave pulses produced by the PSG do not result in as much of a "kick" to the north-south inter-area oscillation as do the Chief Joseph Brake Pulses. There were additional tests conducted in both closed loop and open loop damping controller operation on 29 Sept. 2016. Since results were very similar to the above tests, these plots are not discussed in this paper.

Figs. 14-16 illustrate the responses to the square wave pulses from the PSG for inter-area oscillations, north and south grid frequencies, and PDCI power output, respectively, in both open and closed loop damping control operation. For the power flow on the PDCI depicted in Fig. 16, similar to Fig. 13, the closed-loop plot shows the addition of the PDCI power flow and the commanded power modulation dispatched to the PDCI. The open-loop plot shows only the PDCI power flow since the commanded power modulation dispatched to the PDCI is zero in open-loop operation.

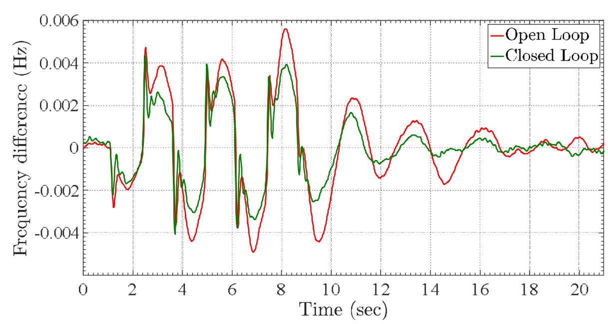

Fig. 14. Frequency difference between north and south PMU locations in open and closed loop control operation during a square-wave pulse insertion on 29 Sept. 2016.

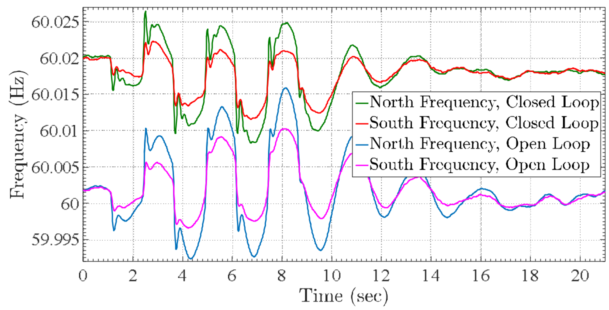

Fig. 15. Bus frequencies from north and south PMU locations in open and closed loop operation during a square-wave pulse insertion on 29 Sept. 2016.

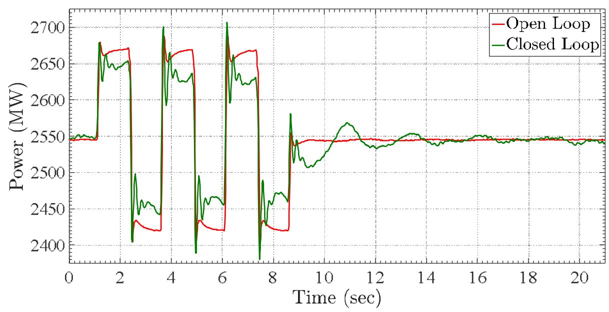

Fig. 16. The power flow on the PDCI during a square-wave pulse insertion on 29 Sept. 2016.

6. CONCLUSIONS AND FUTURE RESEARCH

The design and implementation of a damping controller based on HVDC modulation and real-time PMU feedback is described in this paper. The closed-loop test results show that damping of the primary north-south mode improved by 4.5 percentage points over the open-loop tests. Additional tests also show improved damping in closed-loop vs. open-loop control operation. In all the tests conducted, there was no instance of the damping controller causing harm to the grid. The benefits that the control system is capable of delivering, once operational, include: (1) Additional reliability to the grid through improved damping of electromechanical oscillations. (2) An additional contingency to the grid in a stressed system condition. (3) Higher power capacity on specific transmission corridors. (4) Reduction in the need for new transmission capacity expansion.

New design features and significant additional testing will be necessary before the controller can be deployed in an operational status on the grid. Specific design features to be investigated include the estimation of open-loop gain and phase margins of the grid as a means to monitor damping effectiveness and margins of stability safety. In addition, the incorporation of a deadzone in the modulated power command may reduce high frequency noise in the PDCI power flow. However, this feature must be studied to ascertain any degradation in damping performance.

ACKNOWLEDGEMENTS

The authors gratefully acknowledge the financial support of the Office of Technology Innovation at BPA (Dr. Dmitry Kosterev, technical POC, and Dr. Jisun Kim, project manager) and the substantial efforts of BPA engineers in the project, Mr. Tony Faris, Mr. Jeff Barton, Mr. Michael Overeem, Mr. Greg Stultz, and Mr. Daniel Goodrich. The authors also acknowledge colleagues at Sandia National Laboratories, Mr. Ryan Elliott, Dr. Raymond Byrne, and Dr. Jason Neely for their excellent work on the project. Finally, the authors gratefully acknowledge the financial support and encouragement of the U.S. DOE/OE, specifically, Mr. Phil Overholt, manager of the Transmission Reliability Program, and Dr. Imre Gyuk, manager of the Energy Storage Program.

REFERENCES

Cresap, R.L., Mittelstadt, W.A., Scott, D.N., and Taylor, C.W. (1978). Operating experience with modulation of the Pacific HVDC Intertie. *IEEE Trans. Power Apparatus and Syst.*, vol. 97, no. 4, pp. 1053-1059.

Kosterev, D.N., Taylor, C.W., and Mittelstadt, W.A. (1999). Model validation for the August 10, 1996 WSCC system outage. *IEEE Trans. Power Syst.*, vol. 14, pp. 967–979.

Kundur, P. (1994). *Power System Stability and Control.* McGraw Hill, New York City, NY, USA.

Pierre, B.J., Elliott, R.T., Schoenwald, D.A., Neely, J.C., Byrne, R.H., Trudnowski, D.J., and Colwell, J. (2016). Supervisory system for a wide area damping controller using PDCI modulation and real-time PMU feedback. *2016 IEEE Power and Energy Soc. General Meeting.* IEEE, Boston, MA, USA.

Pierre, B.J., Wilches-Bernal, F., Elliott, R.T., Schoenwald, D.A., Neely, J.C., Byrne, R.H., and Trudnowski, D.J. (2017). Open-loop testing results for the Pacific DC Intertie wide area damping controller. Submitted to *PowerTech 2017*. IEEE, Manchester, UK.

Shelton, M.L., Mittelstadt, W.A., Winkelman, P.F., and Bellerby, W.J. (1975). Bonneville Power Administration 1400 MW Braking Resistor. *IEEE Trans. on Power Apparatus and Systems*, vol. 94, no. 2, pp. 602-611.

Stahlhut, J.W., Browne, T.J., Heydt, G.T., and Vittal, V. (2008). Latency viewed as a stochastic process and its impact on wide area power system control signals. *IEEE Trans. Power Syst.*, vol. 23, no. 1, pp. 84–91.

Trudnowski, D.J. and Pierre, J.W. (2009). Signal processing methods for estimating small-signal dynamic properties from measured responses. In *Inter-area Oscillations in Power Systems: A Nonlinear and Nonstationary Perspective*, Chapter 1. Springer, Berlin, Germany.

Trudnowski, D.J. and Undrill, J. (2009). Modal and Controllability Analysis of the MiniWECC System Model. Year 2 report of BPA contract 37508. Bonneville Power Administration, Portland, OR, USA.

Trudnowski, D.J., Kosterev, D.N., and Undrill, J. (2013). PDCI damping control analysis for the western North American Power System. *2013 IEEE Power and Energy Soc. General Meeting.* IEEE, Vancouver, BC, Canada.

Trudnowski, D.J., Kosterev, D.N., and Wold, J. (2014). Open-loop PDCI probing tests for the western North American Power System. *2014 IEEE Power and Energy Soc. Gen. Meeting.* IEEE, National Harbor, MD, USA.

Wingert, K. (2016). BPA puts modernized Celilo Converter Station into service. BPA News Release, PR 03-16. Bonneville Power Administration, Portland, OR, USA.